Adv. Polar Upper Atmos. Res., **16**, 146-156, 2002

New auroral spectrometer using an acousto-optic tunable filter

Kazuo Shiokawa[1], Yasuo Katoh[1], Mitsugi Satoh[1], Tadahiko Ogawa[1], Makoto Taguchi[2] and Hisao Yamagishi[2]

[1]*Solar-Terrestrial Environment Laboratory, Nagoya University, Honohara, Toyokawa 442-8507*
[2]*National Institute of Polar Research, Kaga 1-chome, Itabashi-ku, Tokyo 173-8515*

Abstract: This paper reports the performance and capability of a newly developed zenith spectrometer (for measurements of airglow and aurora) that uses an acousto-optic tunable filter (AOTF). The AOTF can scan the pass-band of the spectrometer between 450 and 700 nm with a bandwidth of 2-3 nm by changing the RF driver frequency from 180 to 100 MHz. The absolute sensitivity of the spectrometer is ~0.1-1.5 counts/Rayleigh/s per spectral step. The spectrometer is fully automated. The OI (557.7 nm) airglow line can be clearly identified in test observations of midlatitude airglow performed at Shigaraki Observatory, Japan. Based on an estimate of the signal-to-noise ratio, we conclude that the full auroral spectrum (450-700) nm can be measured by the AOTF spectrometer with a time resolution of ~100 s and a signal-to-noise ratio of ~100 for an auroral emission intensity of 10 kR. An example of the auroral spectra is shown for observations made at Syowa Station in Antarctica.

1. Introduction

The utility of noncollinear acousto-optic tunable filters (AOTFs) for performing spectral measurements has been demonstrated by many researchers over the past two decades (*e.g.*, Chang, 1974, 1977; Sivanayagam and Findlay, 1984; Glenar *et al.*, 1994). AOTFs can be used for spectral measurements from 400 nm to more than 2.5 μm. The devices are solid-state, radio frequency (RF) tunable and are composed mostly of tellurium dioxide (TeO_2) materials.

Figure 1 shows the basic geometry of the AOTF. Incident light passing through the RF-driven AOTF is separated into three beams: (A) a horizontally polarized diffracted beam, (B) a nonpolarized undiffracted beam, and (C) a vertically polarized diffracted beam. Because the acoustic waves propagating in the AOTF work as a grating filter, only a limited bandwidth of 2-3 nm is diffracted into (A) and (C). The wavelength diffracted by the AOTF can be controlled by changing the RF frequency that is transmitted to the AOTF. Thus, the AOTF can be used as a fast-scanning band-pass filter. Moreover, by adjusting appropriate optics and employing a two-dimensional detector, the AOTF can be used as an imaging spectrometer.

Spectral measurements of aurora and airglow have been made mainly using grating

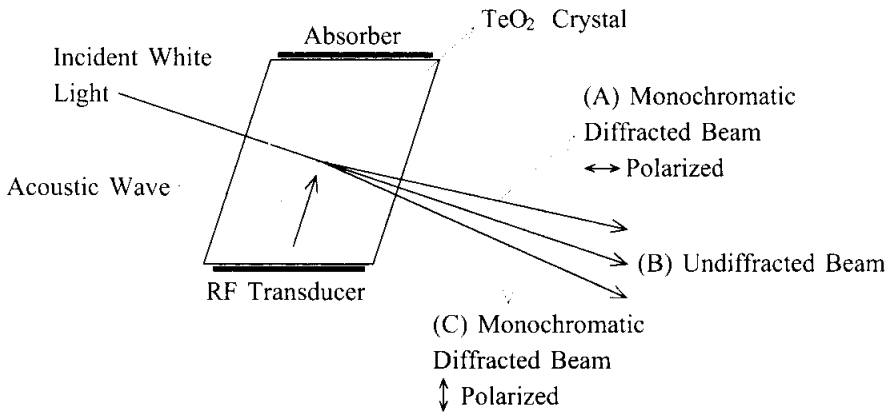

Fig. 1. Schematic diagram showing the basic geometry of the acousto-optic tunable filter.

spectrometers (*e.g.*, Broadfoot and Kendall, 1968; Okamura and Ejiri, 1992; Johnstone and Broadfoot, 1993; Chamberlain, 1995). Despite the above-mentioned unique capabilities of AOTFs, they have never been used as spectrometers for the measurement of polar aurora, mainly because the small aperture of the AOTFs (maximum ~10 mm × 10 mm) results in a small throughput of 2.4×10^{-3} cm^2 sr for a typical aperture angle of 1.6°. However, the fast-scanning and imaging capabilities of the AOTF are attractive for researchers performing spectral measurement of aurora and other intense atmospheric emissions. In this paper, we report the performance of an AOTF spectrometer that was developed for the measurement of auroral spectra.

2. Instrumentation

Figure 2 shows a schematic diagram of the AOTF spectrometer system. The specifications of the AOTF are listed in Table 1. The AOTF and the RF driver were made by Brimrose Corporation (USA). We developed the appropriate optics and software for the photometer. The optics consists of three identical achromats, each with a focal length of 30 mm and a diameter of 25 mm. The total angle of incident light entering the AOTF is limited to 2.5° by the circular field stop at the first focal point. This almost-parallel incident light provides sufficient separation of the diffracted and undiffracted light spots on the final focal plane. The field-of-view of the front lens is set at 2.5°. The incident light from the front lens passes through the AOTF, which has an aperture of 10 mm × 10 mm, and is focused on a photomultiplier tube (Hamamatsu R649). The spectrometer is fairly compact, measuring ~500 mm (height) × 150 mm (width) × 150 mm (depth).

The photon counts from the photomultiplier are sent to a personal computer through a 30-m signal cable and are recorded onto a hard disk. The shutter just above the field stop is controlled by the personal computer; as a fail-safe system, the shutter is designed to remain closed when daylight is detected by a CdS optical sensor. The personal computer enables the system to be operated automatically by controlling the photon counter, shutter driver, and RF frequency and power of the AOTF driver. The whole system is backed

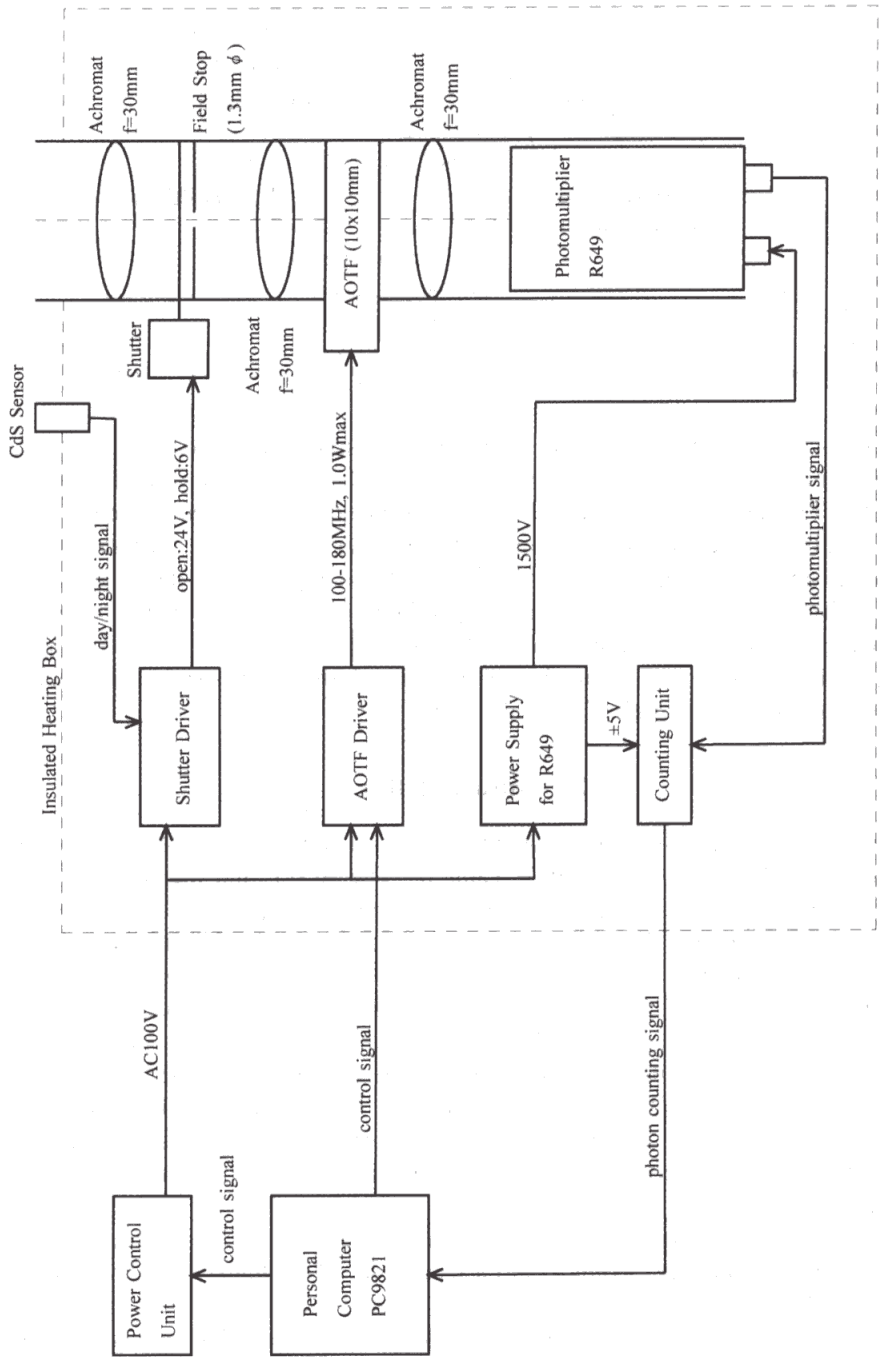

Fig. 2. Schematic diagram of the AOTF spectrometer system.

Table 1. Specifications of the acousto-optic tunable filter used for the spectrometer.

Item	Specification
Wavelength range	450–700 nm
Optical aperture	10×10 mm
Angular aperture (total angle)	3.2°–4.5°
Separation angle	7°–6°
Spectral resolution	0.8 nm at 450 nm
	3.0 nm at 700 nm
Peak diffraction efficiency	60%
RF frequency range	180–100 MHz
RF power	1.0–1.5 W
Frequency sweeping speed	15 ms (type) from 180 to 100 MHz

up by a power supply (not shown) that can run for more than 10 min in the event of a power failure.

The diffraction of the AOTF produces three light spots on the final focal plane of the photomultiplier tube. To measure the intensity of the monochromatic diffracted light, the undiffracted center spot is masked with a metal plate so that only the two diffracted spots are detected. The diffraction angle is constant independent of the wavelengths of the diffracted beams. The two side spots have a 90° difference in polarization but can not be distinguished from each other on the photomultiplier tube.

3. Calibration

As listed in Table 1, the AOTF has a scanning range of 450–700 nm with a spectral resolution of 0.8 nm (at 450 nm) to 3.0 nm (at 700 nm); the desired scanning range and spectral resolution can be obtained by changing the RF drive frequency from 180 to 100 MHz. We have divided this frequency range into 250 equal steps. The center wavelength, absolute sensitivity, and bandwidth of the spectrometer for these 250 steps are shown in Fig. 3. These calibrations were performed out using a 2-m integrating sphere and a monochromatic light source at the National Institute of Polar Research, Japan. The sensitivities in Fig. 3 were obtained by measuring white light from the integrating sphere, the brightness of which was known. The center wavelength and bandwidth were obtained by measuring monochromatic light with a bandwidth of 0.1 nm for every 0.5-nm step between 450 nm and 700 nm.

A quasi-linear relation between the RF frequency and the center wavelength can be seen in Fig. 3. The fluctuations in sensitivity and bandwidth occur because the spectral resolution of the calibration for determining the transmission function was relatively low (0.5 nm) compared to the band width (2–3 nm). In any case, the sensitivity decreases from 1.5 counts/R/s to 0.1 counts/R/s (per spectral step) and the bandwidth increases from ~2 nm to ~3 nm as the center wavelength increases from 450 nm to 700 nm.

The total angle of the incident light that passes through the AOTF was set at 2.5°. This sets the total throughput $A\Omega$ of the optics at $A\Omega = 2\pi(1-\cos(1.25°))\times 1 = 1.5\times 10^{-3}$ sr cm^2, where A and Ω are the area (1 cm^2) and the solid angle (sr) of the light that passes through the AOTF, respectively. Assuming that the total transmission T of the optics,

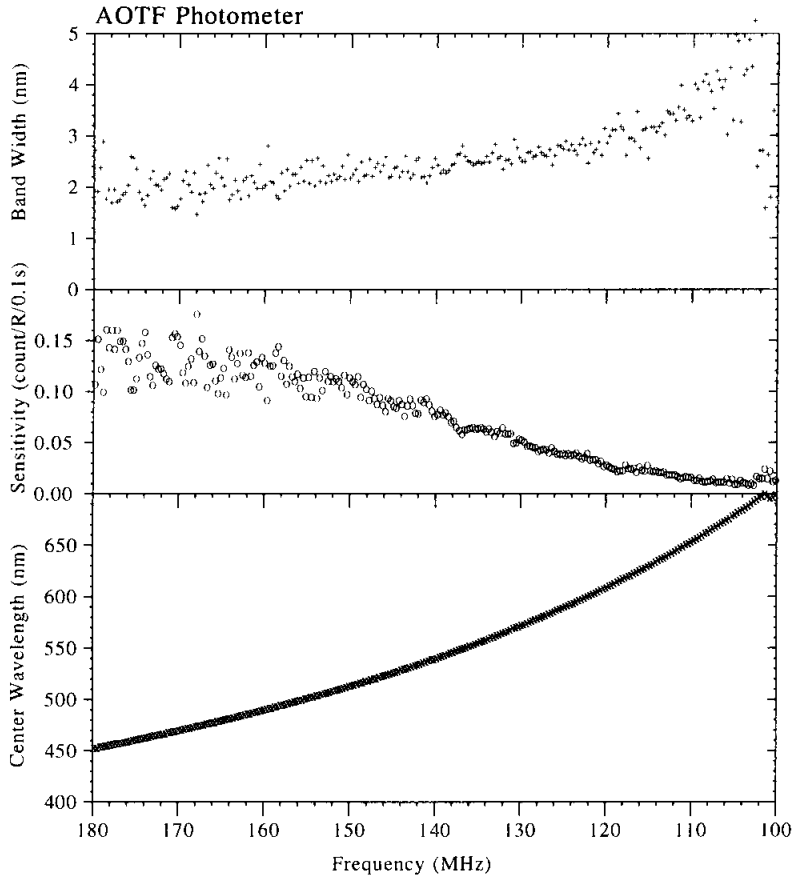

Fig. 3. Center wavelength, absolute sensitivity, and bandwidth of the AOTF spectrometer for each RF frequency imposed on the AOTF.

including the diffraction efficiency of the AOTF, is 0.5 and the quantum efficiency q of the photomultiplier tube is 0.15 at a wavelength of 400 nm, the ideal sensitivity $S=(10^6/4\pi)$ $A\Omega Tq$ becomes 8.8 counts/R/s. This value is about 6 times larger than the actual value (1.5 counts/R/s) obtained by the calibration.

We have yet to discover the cause of this discrepancy, but several factors can reduce the ideal sensitivity. First, creating an appropriate optical mask that allows the two diffracted beams to pass and blocks the undiffracted center beam is quite difficult. To avoid contamination from the intense undiffracted beam, the two holes on the optical mask are slightly smaller than the theoretically optimal diameter. A second possible reason for the above discrepancy is that the quantum efficiency of the photomultiplier tube (R649) may be smaller than the expected value because of the non-uniformity of the photoelectric surface. We had to use the area around the edge of the photoelectric surface (8 mm$\times$5 mm) of R649. Because the two diffracted light spots are separated by about 8 mm, the area around the edge of the photoelectric surface of R649 (8 mm$\times$5 mm) had to be used. These problems could be avoided by using imaging detectors, such as cooled-CCDs, at the

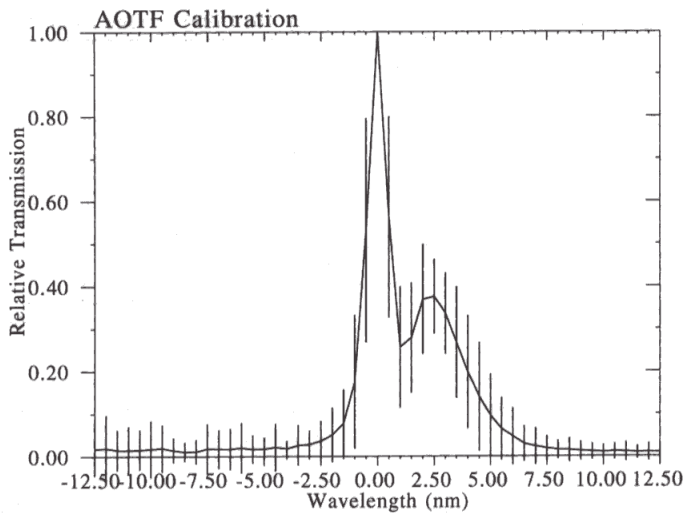

Fig. 4. Transmission function of the AOTF spectrometer normalized by both the center wavelength and the peak transmission. This function was obtained by averaging all the transmission functions for 250 frequency steps. The vertical bars indicate the standard deviations.

final focal plane.

Figure 4 shows the average transmission function of the AOTF photometer. This function is obtained by averaging all the transmission functions for the 250 frequency steps and normalized by both the center wavelength and the peak transmission. The vertical bars indicate the standard deviations. A sub-peak transmission about 2.5 nm away from the transmission center (towards the longer wavelength) can be clearly seen in this figure. This sub-peak probably produced by a power overdrive. The RF power used to drive the AOTF might be too strong. If so, this would explain why the measured bandwidth in Fig. 3 is larger than the expected instrumental specification listed in Table 1. Unfortunately, the airglow and auroral measurements performed in Japan and the Antarctica that are described below were performed under this overdrive situation producing broader bandwidths. Further calibrations are necessary to determine the optimal RF power.

4. Observations

We used the AOTF spectrometer described in the present report to observe mid-latitude nocturnal airglow at Shigaraki Observatory (34.8°N, 136.1°E), Kyoto University, in July 1999 and Antarctic aurora at the Syowa Station (69.0°S, 39.6°E, magnetic latitude: −70.3°) between February–October 2000. The airglow and auroral spectra were obtained by scanning the RF frequency from 180 to 100 MHz in 250 equal steps. The exposure time of each step was 0.1 s. Thus, one spectrum was obtained every 25 s. However, the spectrum had to be further averaged because of the noise produced by the photomultiplier tube. The averaging interval varied according to the signal intensity.

Figure 5 shows an example of a zenith airglow spectrum measured at Shigaraki on

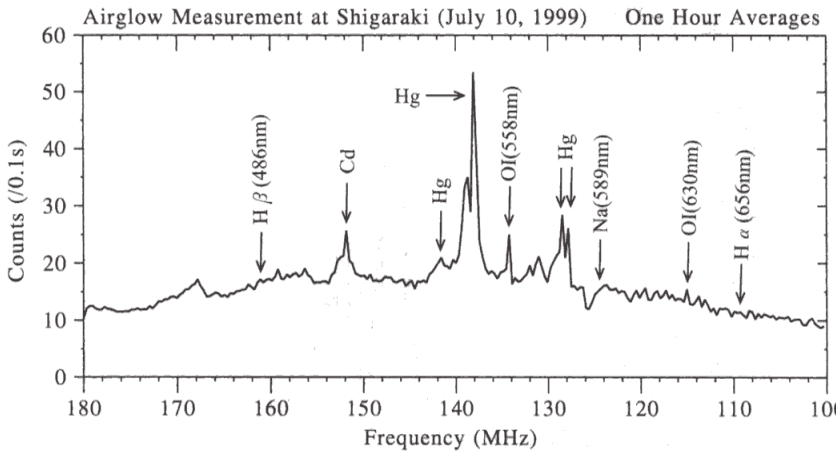

Fig. 5. Zenith airglow spectrum measured by the AOTF spectrometer between 1115 and 1215 UT (2015–2115 LT) on July 10, 1999, at the Shigaraki Observatory, Japan. Data obtained from 144 scans (one hour) were averaged. Several lines from city lights (Mercury and Cadmium) and two OI airglow lines (557.7 nm and 630.0 nm) can be identified. The expected locations of other airglow and auroral lines (Hα, Hβ, and Na) are also shown.

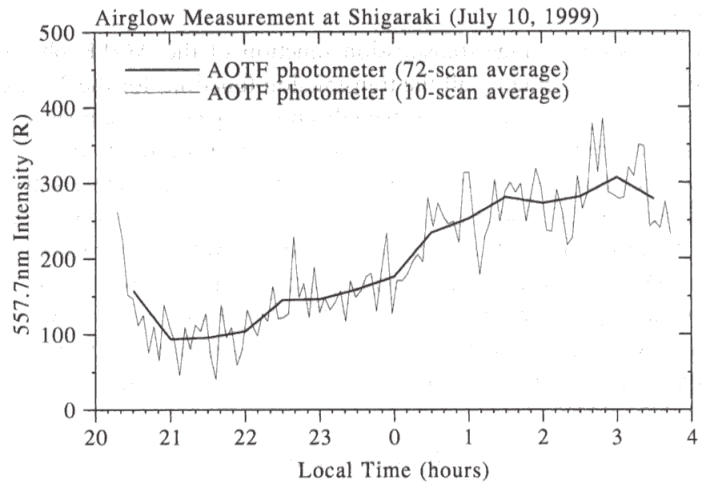

Fig. 6. Variation in OI (557.7 nm) airglow intensity measured by the AOTF spectrometer on July 10–11, 1999, at the Shigaraki Observatory. The heavy and light curves are the intensities obtained by averaging 72 scans (7.2-s exposure) and 10 scans (1.0-s exposure), respectively. The data shown by these curves were obtained every 30 min and 250 s, respectively, because one full scan over the 450–700 nm range requires 25 s. Background sky emissions and dark counts were subtracted from the plotted data using data for a neighboring wavelength.

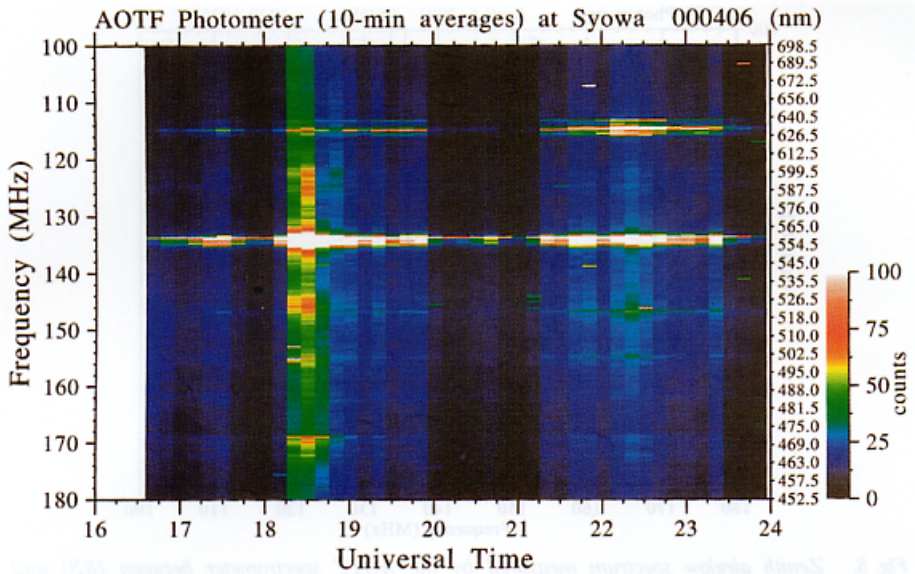

Fig. 7. Time sequence of zenith auroral spectra measured by the AOTF spectrometer between 1630 and 2400 UT (1930–0300 LT) during a magnetic storm on April 6, 2000, at the Syowa Station, Antarctica. Spectral data averaged over 24 scans (10 min) were used.

July 10, 1999, averaged over one hour (=25 s×144 scans). Intense mercury emission lines are identified. These lines probably originated from a light source in an observatory building that was located bout 200 m away from the spectrometer. Airglow lines at OI 557.7 nm and 630.0 nm are in the spectrum, but the sodium (Na) line at 589.3 nm is indistinct. The 144-scan average produced a noise level of ~2 counts (rms), as can be seen in the figure.

Using the calibration parameters shown in Fig. 3, we calculated the variations in absolute intensity of the O I (557.7 nm) line for this night. The result is shown in Fig. 6. The intensity increases from ~100 R to ~300 R between 21 LT and 03 LT. Background sky emissions were subtracted from the data by using the counts for a neighboring step. The noise level of the 10-scan average data was ~50 R (rms). The 72-scan average (72× 25 s=30 min), which corresponds to an exposure time of 7.2 s per step, produces a reasonable curve for airglow variation in the 100–300 R intensity range.

Figure 7 shows the dynamic spectrum (24 scans=10-min averages) of auroral emissions measured on April 6, 2000, at Syowa Station, Antarctica. An intense magnetic storm started at 1639 UT on this day. The maximum *Dst* index (provisional) was −321 nT at 0100 UT on April 7. An intense green line (557.7 nm) was observed throughout the observation. The intensity of the emissions peaked at between 1800–1900 UT (2100–2200 LT). The red line (630 nm) was enhanced at around 2200–2300 UT (0100–0200 LT). Several pictures of a spectacular red aurora were taken around this time. It should be noted in this figure that when the auroral emission lines were enhanced, the background continuum emission was also enhanced (*e.g.*, 1800–1900 UT). The reason for this is

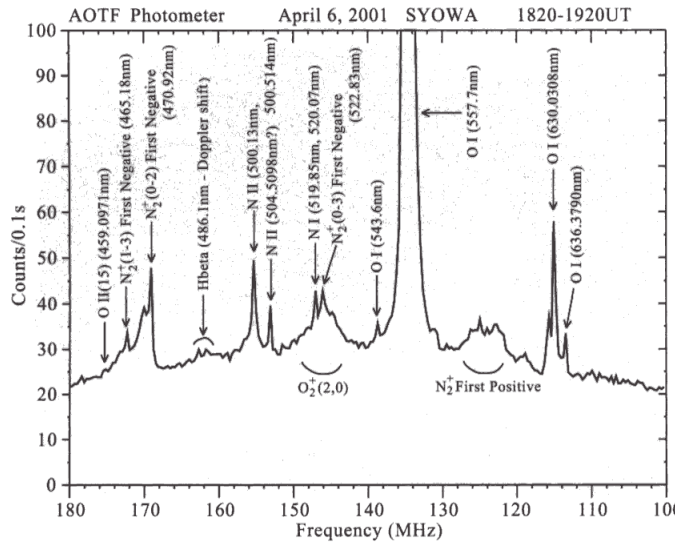

Fig. 8. Zenith airglow spectrum measured by the AOTF spectrometer between 1820 and 1920 UT (2120–2220 LT) during a magnetic storm on April 6, 2000, at the Syowa Station, Antarctica. Data obtained from 144 scans (one hour) were averaged. Many auroral lines, including O I (557.7 nm and 630.0 nm), can be identified.

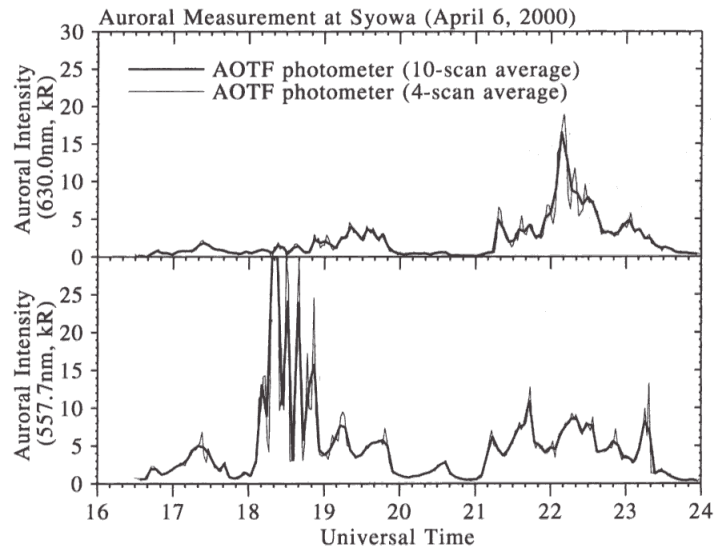

Fig. 9. Variations in OI (557.7 nm and 630.0 nm) auroral intensity measured by the AOTF spectrometer on April 6, 2000, at the Syowa Station, Antarctica. The heavy and light curves are the intensities obtained by averaging over 10 scans (1.0-s exposure) and 4 scans (0.4-s exposure), respectively. The data shown by these curves were obtained every 250 and 100 s, respectively, since one full scan over 450–700 nm range requires 25 s. Background sky emissions and dark counts were subtracted from the plotted data using data for a neighboring wavelength.

probably that the measured spectrum was contaminated by zero-order undiffracted emissions arising from multiple scattering in the optics.

The spectrum of the most intense auroral emission at 1820–1920 UT (2120–2220 LT, averaged over one hour = 144 scans) is shown in Fig. 8. Various auroral emission lines and bands can be identified in this spectrum, as indicated. Because of the sub-peak of the filter transmission, shown in Fig. 4, the spectral separation is not very good. For example, the two OI emissions at 630.0 nm and 636.4 nm partially overlap.

Similar to the airglow measurements at Shigaraki, we also calculated the variations in absolute intensity of the OI (557.7 nm and 630.0 nm) on this night. The result is shown in Fig. 9. Background sky emissions were subtracted using the counts for a neighboring step. Thus, the absolute intensity calculation was not affected by the contamination of the zero-order undiffracted beam. The green line (557.7 nm) reached its peak intensity at 1800–1900 UT, while the intensity of the red line (630.0 nm) exceeded that of the green line at around 2200 UT. The figure clearly shows that a 4-scan average (4×25 s = 100 s temporal resolution) already produces a reasonable curve of auroral intensity variation. For example, the curve does not show noise fluctuations at around 20–21 UT, even when the auroral intensity is small.

5. Summary and discussion

We have constructed a compact zenith spectrometer that uses an acousto-optic tunable filter with a wavelength range of 450–700 nm. The bandwidth and sensitivity of the spectrometer are 2–3 nm and 0.1–1.5 counts/R/s/step, respectively. We found that an overdrive of the RF signal causes the bandwidth to broaden with a sub-peak occurring in the transmission function. The spectrometer is automatically operated by a personal computer. Test observations of midlatitude airglow indicate that variations in airglow intensity of a few hundred R can be measured using an exposure time of 7.2 s (72-scan average = 30-min temporal resolution). Automatic measurements of an aurora were performed using the spectrometer at Syowa Station between February and October 2000. Various auroral spectra were obtained from the observations.

One set of full-scan data is obtained every 25 s using an exposure time of 0.1 s/step. This value sets the minimum time resolution of the spectral measurement. Depending on the intensity of the aurora, the averaging time interval can be varied in multiples of 25 s. As shown in Fig. 8, various auroral emission lines are included in the range of measured wavelengths. The auroral emission intensity is much greater than that of airglow. The estimated noise level is 2 counts for 144 scan averages, as shown in Fig. 5. This means that the noise level per scan is 24 counts/0.1 s/step ($=2 \times \sqrt{144}$). For the 10-kR auroral emission, the output was 1000 counts/0.1 s/step for a sensitivity of 1.0 counts/R/s/step. Thus, a 4-scan (100 s) average produces a signal-to-noise ratio of ~ 100 ($= 1000/(24/\sqrt{4})$). For the actual measurement shown in Fig. 9, a temporal resolution of 100 s seems to be sufficient to measure variations in intensity of more than 1 kR.

Since the personal computer can arbitrary change the RF frequency, the program can be set to only select the frequencies that correspond to auroral emission lines. In this situation, the actual time resolution becomes much better than that of a full scan.

The automatic operation of the AOTF spectrometer is fairly stable because the

spectrometer does not have any moving parts (for wavelength scans). The AOTF can arbitrary change the center wavelength. These characteristics are suitable for future space-borne measurements of aurora and other atmospheric emissions. Recently, considerable progress has been made in the construction of a highly sensitive imaging detector using cooled-CCD devices. By combining this detector with the AOTF, the spectrometer could be used for imaging spectroscopy of aurora.

Acknowledgments

We would like to gratefully acknowledge T. Katoh of the Solar-Terrestrial Environment Laboratory, Nagoya University, for his skillful support in the construction of the spectrometer hardware. H. Fukunishi and Y. Takahashi of Tohoku University provided the suggestion of using an acousto-optic tunable filter as a spectrometer. The spectrometer was calibrated using the facilities at the National Institute of Polar Research, Japan. Test observations at Shigaraki Observatory were performed out in collaboration with the Radio Science Center for Space and Atmosphere of Kyoto University. The authors wish to thank the members of the 41st Japanese Antarctic Research Expedition for their various support in performing the auroral observations at Syowa Station. This work was supported by a Grant-in-Aid from the Ministry of Education, Culture, Sports, Science, and Technology of Japan (11440145).

The editor thanks Dr. T. Aso for his help in evaluating this paper.

Reference

Broadfoot, A.L. and Kendall, K.R. (1968): The airglow spectrum, 3100-10000 A. J. Geophys. Res., **73**, 426-428.

Chamberlain, J.W. (1995): Physics of the aurora and airglow. Classics in Geophysics, Washington, D.C., American Geophysical Union.

Chang, I.C. (1974): Noncollinear acousto-optic filter with large angular aperture. Appl. Phys. Lett., **25**, 370-372.

Chang, I.C. (1977): Tunable acousto-optic filters: An overview. Opt. Eng., **16**, 455-460.

Glenar, D.A., Hillman, J.J., Saif, B. and Bergstralh, J. (1994): Acousto-optic imaging spectropolarimetry for remote sensing. Appl. Opt., **33**, 7412-7424.

Johnstone, J.E. and Broadfoot, A.L. (1993): Midlatitude observations of the night airglow: Implications to quenching near the mesopause. J. Geophys. Res., **98**, 21593-21603.

Okamura, H. and Ejiri, M. (1992): A new imaging spectrometer for the auroral spectroscopic studies. J. Geomagn. Geoelectr., **44**, 193-205.

Sivanayagam, A. and Findlay, D. (1984): High resolution noncollinear acoustooptic filters with variable passband characteristics: Design. Appl. Opt., **23**, 4601-4608.

(Received February 1, 2002; Revised manuscript accepted April 18, 2002)